DOI: 10.1002/adsc.201700202

Advanced Synthesis & Catalysis

Metal Substitution Modulates the Reactivity and Extends the Reaction Scope of Myoglobin Carbene Transfer Catalysts

Gopeekrishnan Sreenilayam,[+a] Eric J. Moore,[+a] Viktoria Steck,[a] and Rudi Fasan[a,*]

[a] Department of Chemistry, University of Rochester, Rochester, New York 14627, USA
Fax: (+1)-585-276-0205; phone: (+1)-585-273-3504; e-mail: rfasan@ur.rochester.edu

[+] These authors contributed equally to this work.

Received: February 16, 2017; Revised: April 11, 2017; Published online: May 15, 2017

Supporting information for this article can be found under https://doi.org/10.1002/adsc.201700202.

Abstract: Engineered myoglobins have recently emerged as promising scaffolds for catalyzing carbene-mediated transformations. In this work, we investigated the effect of altering the metal center and first-sphere coordination residue on the carbene transfer reactivity of myoglobin. To this end, we first established an efficient protocol for the recombinant expression of myoglobin variants incorporating metalloporphyrins with non-native metals, including second- and third-row transition metals (ruthenium, rhodium, iridium). Characterization of the cofactor-substituted myoglobin variants across three different carbene transfer reactions (cyclopropanation, N–H insertion, S–H insertion) revealed a major influence of the nature of the metal center, its oxidation state and first-sphere coordination environment on the catalytic activity, stereoselectivity, and/or oxygen tolerance of these artificial metalloenzymes. In addition, myoglobin variants incorporating manganese- or cobalt-porphyrins were found capable of catalyzing an intermolecular carbene C–H insertion reaction involving phthalan and ethyl α-diazoacetate, a reaction not supported by iron-based myoglobins and previously accessed only using iridium-based (bio)catalysts. These studies demonstrate how modification of the metalloporphyrin cofactor environment provides a viable and promising strategy to enhance the catalytic properties and extend the reaction scope of myoglobin-based carbene transfer catalysts.

Keywords: artificial metalloenzymes; biocatalysis; carbene transfer; C–H carbene insertion; myoglobin; protein engineering

Introduction

The transition metal-catalyzed insertion of carbenoid species into C=C, Y–H (Y=N, S, O, Si), and C–H bonds constitutes a powerful approach to the construction of new carbon-carbon and carbon-heteroatom bonds in organic chemistry.[1] While major efforts have been devoted to the development of organometallic complexes for executing these transformations,[1] biocatalytic platforms useful for promoting carbene transfer reactions have only recently begun to emerge.[2] Arnold and co-workers have shown how cytochrome P450 enzymes can catalyze the cyclopropanation of styrene derivatives and carbene N–H insertion with aniline derivatives.[3] Our group has demonstrated how engineered myoglobins can promote a wide range of carbene-mediated transformations, including olefin cyclopropanation,[4] carbene N–H and S–H insertions,[5] aldehyde olefination,[6] and [2,3]-sigmatropic rearrangement reactions.[7] More recently, biocatalytic systems based on these[8] and other protein and DNA scaffolds have been investigated in the context of carbene transfer reactions.[9]

Myoglobin (Mb) contains a heme cofactor (=iron-protoporphyrin IX), which is embedded within the core of the protein *via* non-covalent interactions and coordination of the iron atom through the side-chain imidazolyl group of a "proximal" histidine residue (His93 in sperm whale myoglobin).[10] During myoglobin-mediated carbene transfer catalysis, the α-diazoester carbene donor reagents are predicted to react with the heme center to give rise to a reactive heme-bound carbenoid intermediate.[4a] This species has electrophilic character[4a] and can engage a variety of nucleophilic substrates in a reaction manifold that leads to the formation of cyclopropanes,[4a] amines,[5a] thioethers,[5b,7] and olefins.[6] Under this mechanistic scenario, we hypothesized that the nature of the

metal center as well as the presence/absence of first-sphere coordination *via* the proximal histidine residue could have a significant influence on the carbene transfer reactivity of these biocatalysts. In this work, we have investigated this aspect through the preparation of metal- and proximal ligand-substituted myoglobin variants and the characterization of their activity in a series of model carbene insertion reactions under varying reaction conditions. To enable these studies, we first implemented an efficient strategy for the recombinant production of myoglobin variants incorporating first-, second- and third-row transition metals in bacterial cells. Our results show how metal and proximal ligand substitution provides an effective means to (a) modulate the catalytic activity, selectivity, and oxygen tolerance of these myoglobin-based catalysts toward different types of carbene-mediated transformations and (b) extend the reaction scope of these carbene transfer biocatalysts to include intermolecular carbene C–H insertion reactivity.

Results and Discussion

Recombinant Expression of Cofactor-Substituted Myoglobins

Pioneering studies by Yonetani, Hayashi and Watanabe have demonstrated the possibility to substitute the heme cofactor in myoglobin with non-native metalloporphyrins and porphynoids.[11] These strategies have involved extraction of the heme from the protein with organic solvents followed by dialysis and refolding of apomyoglobin (=heme-free myoglobin) in the presence of the non-native cofactor. More recently, Watanabe and co-workers reported the successful preparation of metallo-substituted hemoproteins *via* reconstitution of apo-hemoproteins with metalloporphyrins directly in cell lysate,[12] whereas a related protocol was applied by Hartwig and co-workers to obtain various metallo-substituted myoglobins, although only Ir-containing variants were isolated and characterized.[8a] Despite this progress, *in vitro* reconstitution protocols tend to be laborious and time-consuming, requiring extensive manipulation of the protein after expression and purification. In addition, they are incompatible with the realization of biocatalytic transformations using whole-cell systems.[4b]

To overcome these limitations, our group has investigated strategies to enable the recombinant production of metal- and cofactor-substituted hemoprotein-based catalysts. To this end, we previously developed and reported an efficient protocol for the recombinant production of Mn- and Co-containing Mb, which relies on the use of *E. coli* cells expressing a heterologous outer membrane heme transporter (ChuA)[13] and the chaperone complex GroEL/ES.[14] In this system, ChuA mediates the cellular uptake of exogenous Mn- and Co-protoporphyrin IX [Mn(ppIX) and Co(ppIX), respectively] supplemented to the growth medium. Cells are grown in iron-free minimal medium to prevent the production of heme. Co-expression of the chaperone proteins GroEL/ES was found to increase the expression levels of soluble cofactor-substituted Mb, possibly by reducing aggregation of apomyoglobin prior to binding to the non-native cofactor.[14] While these and other studies suggested a certain permissivity of the ChuA transporter toward the uptake of heme analogs containing first-row transition metals,[9c,14,15] its functionality in the context of metalloporphyrin complexes containing second- and third-row transition metals remained to be determined.

Given the promising activity of synthetic Ir(Me)-porphyrins as carbene transfer catalysts,[16] we initially targeted the preparation of Mb incorporating Ir(Me)-protoporphyrin IX [Ir(Me)(ppIX), **3a**]. The latter was prepared in two steps and 22% overall yield *via* metallation of protoporphyrin IX dimethyl ester **1a** with $[Ir(COD)Cl]_2$, followed by methylation with MeI, and ester hydrolysis (Scheme 1A, see the Supporting Information for further details). Upon optimization of the expression conditions, Mb[Ir(Me)(ppIX)] was successfully produced and isolated from *E. coli* in good yields (3.5 mg L^{-1} culture). The electronic absorption spectrum of this protein shows a Soret band at 399 nm prior to and after addition of dithionite, which differs from the characteristic Soret signatures of ferric and ferrous Mb at 410 and 434 nm, respectively (Figure 1A). Furthermore, no signal at 424 nm was observed upon addition of reductant and CO to the protein, further confirming the absence of contaminant Mb. These results were achieved upon introducing important modifications to our previously reported expression protocol, including pre-incubation of the cells with the non-native cofactor prior to induction, culture condensation, and optimization of cell induction conditions (see the Experimental Section for further details). The cell condensation strategy also reduces the amount of non-native cofactor required during expression of the Mb variant.

Encouraged by these initial results, we tested the incorporation of Ir(Me)-mesoporphyrin IX [Ir(Me)(mpIX), **3b**], which is structurally analogous to Ir(Me)(ppIX) and synthetically more accessible [48% yield from mesoporphyrin IX dimethyl ester (**1b**); Scheme 1A]. Notably, the Ir(Me)(mpIX) complex could be incorporated into Mb with comparable efficiency to the protoporphyrin IX-based counterpart (5 mg L^{-1} culture). These results thus demonstrated the ability of the ChuA transporter to recognize heme analogs with a modified metal center and porphyrin ligand. Building upon these findings, Mb variants incorporating second-row transition metals in the form

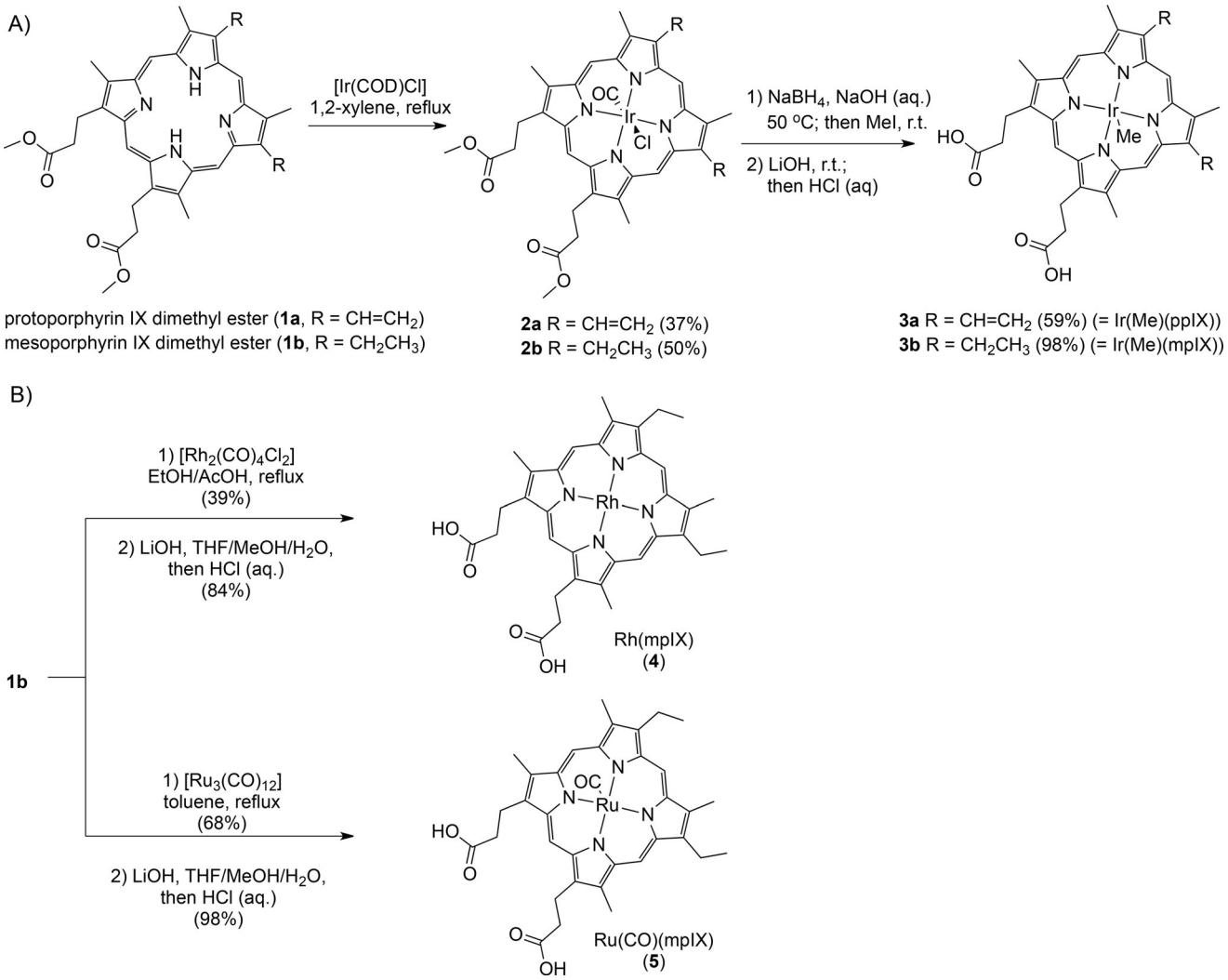

Scheme 1. Synthetic routes for preparation of Ir(Me)-protoporphyrin IX and Ir(Me)-mesoporphyrin IX (A) and Rh- and Ru(CO)-mesoporphyrins IX (B).

of Ru(CO)(mpIX) and Rh(mpIX) (Scheme 1B) were also successfully expressed and isolated from *E. coli* (2–3 mg L^{-1} culture). Based on the amount of apomyoglobin obtained under the same expression conditions in the absence of supplemented cofactor, the efficiency of *in vivo* incorporation of the non-natural metalloporphyrin cofactor was estimated to range between 50% and 90%. Overall, using the strategy outlined above, a panel of Mb catalysts based on the broadly active Mb variant Mb(H64V,V68A)[4a] and containing different metal centers (Mn, Co, Ru, Rh, Ir) was obtained. As expected, each construct exhibits a distinctive spectroscopic signature corresponding to the Soret band and Q bands (Figure 1 and Supporting Information, Table S1). The spectral properties of the recombinantly produced cofactor-substituted Mb variants were identical to those of the corresponding variants obtained *via in vitro* reconstitution with apomyoglobin (see Experimental Section), thus further confirming the efficiency of cofactor incorporation through the recombinant method. Altogether, these experiments demonstrated that the substrate scope of ChuA extends beyond metalloporphyrins based on protoporphyrin IX and first-row transition metals. Importantly, a convenient, time-effective, and technically straightforward strategy was implemented to produce cofactor-substituted Mb catalysts.

Selection of Mb Variants and Carbene Transfer Reactions

We previously identified Mb(H64V,V68A) as a highly active and stereoselective biocatalyst for olefin cyclopropanation.[4a] This Mb variant also possesses high catalytic activity toward other carbene-mediated transformations such as N–H and S–H insertion.[5] Based on these properties, Mb(H64V,V68A) was se-

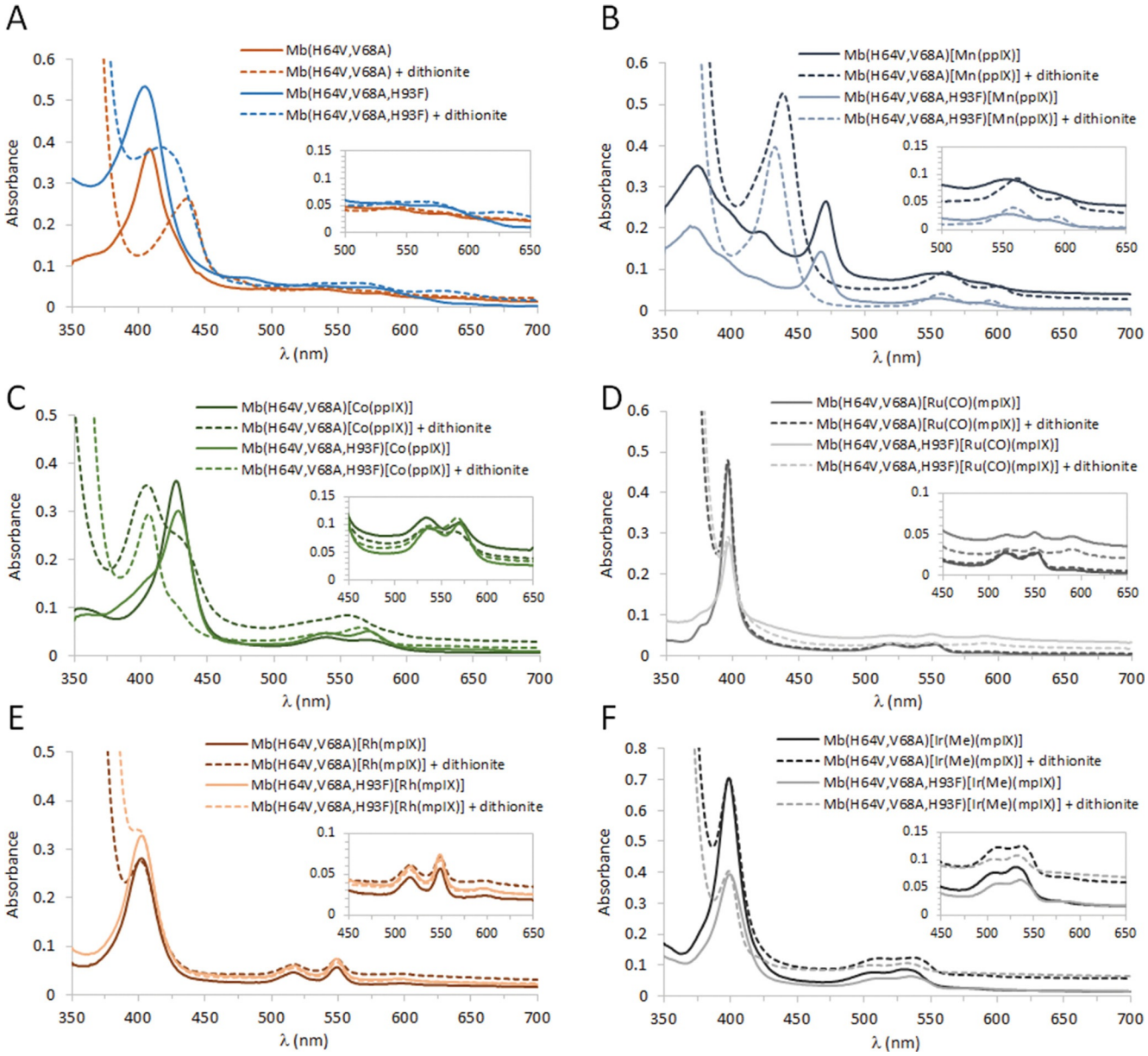

Figure 1. Electronic absorption spectra for Mb(H64V,V68A) and Mb(H64V,V68A,H93F) variants incorporating (**A**) Fe-protoporphyrin IX (heme), (**B**) Mn-protoporphyrin IX, (**C**) Co-protoporphyrin IX, (**D**) Ru(CO)-mesoporphyrin IX, (**E**) Rh-mesoporphyrin IX, and (**F**) Ir(Me)-mesoporphyrin IX, as the cofactor. Spectra were measured prior to (solid line) and after (dashed line) addition of sodium dithionite. The inset plots illustrate the Q band region of each spectrum. See the Supporting Information, Table S1 for further details on the spectroscopic features of these proteins.

lected as an optimal scaffold to examine the impact of metal substitution on Mb-mediated carbene transfer reactivity and stereoselectivity. Accordingly, a first set of cofactor-substituted Mb(H64V,V68A) variants containing a Mn, Co, Ru, Rh, and Ir metal center were prepared as described earlier. A second set of Mb variants was then generated based on the triple mutant Mb(H64V,V68A,H93F), in which the histidine residue involved in axial coordination of the heme iron (His93) is substituted for another aromatic residue which lacks any side-chain Lewis basic group for metal binding (Phe). These proximal ligand Mb variants were meant to provide insights into the functional role of first-sphere metal coordination by the proximal histidine residue on the carbene transfer activity of these metalloproteins. Perturbation of the cofactor environment as a result of the H93F substitution is evidenced by the shift in the Soret bands in the corresponding visible range spectra of these proteins, in particular for those containing first-row metals (Figure 1A–C and Supporting Information, Table S1).

The panel of ten different Mb catalysts (=5 metal centers, with and without H93F substitution) was initially characterized for activity in three model carbene transfer reactions, namely cyclopropanation of styrene, N–H insertion with aniline, and S–H insertion with thiophenol, in the presence of ethyl α-diazoacetate (EDA) as carbene donor. In each case, the reactions were performed in the presence or absence of reductant (sodium dithionite) and under anaerobic and aerobic conditions with the two-fold purpose of (i) evaluating the effect of these parameters on catalyst performance, and (ii) identifying Mb variants capable of operating under aerobic conditions. Indeed, the application of iron-based myoglobins as carbene transfer catalysts has so far required strictly anaerobic conditions, due to the inhibitory action of oxygen, i.e., Mb native ligand, on this non-native reactivity. Oxygen tolerance is desirable as it enhances the accessibility of these biocatalysts for synthetic applications.

Cyclopropanation Activity

Table S2 in the Supporting Information reports the results for the cyclopropanation reactions in the presence of the various Mb catalysts under the four different reaction conditions, with the most relevant data being summarized in Table 1. These reactions were carried out under catalyst-limited conditions to enable a direct comparison of the performance of each Mb variant under these settings. Under "standard conditions" (anaerobic + $Na_2S_2O_4$ or "–/red."), Mb(H64V,V68A) provides a 64% conversion of styrene (**6**) and EDA (**7**) to the *trans*-(1*S*,2*S*) cyclopropane product (**8**) with excellent diastereo- and stereoselectivity (99.9% *de* and *ee*; entry 1, Table 1). Under the same conditions, low product yields (0–7%) were observed for the Mb(H64V,V68A) and Mb(H64V,V68A,H93F)-based variants containing a Co, Rh, or Ru center (entries 5–7, Table 1). Compared to the latter, Mb(H64V,V68A)[Mn(ppIX)] and Mb(H64V,V68A)[Ir(Me)(mpIX)] exhibit noticeably higher cyclopropanation activity, as indicated by the higher yields (29–36% *vs.* 0–7%) and catalytic turnovers (290–356 TON *vs.* 11–68 TON, Supporting Information, Table S2) obtained with these Mb variants under anaerobic conditions (entries 4 and 9, Table 1). Interestingly, Mb(H64V,V68A,H93F)[Mn(ppIX)] showed negligible product conversion (<2%) under identical conditions (Supporting Information, Table S2), indicating that coordination of the manganese center by the proximal histidine residue is critical for cyclopropanation activity. This is contrast to

Table 1. Catalytic activity and selectivity of cofactor-substituted Mb variants for cyclopropanation of styrene with ethyl α-diazoacetate (EDA).[a]

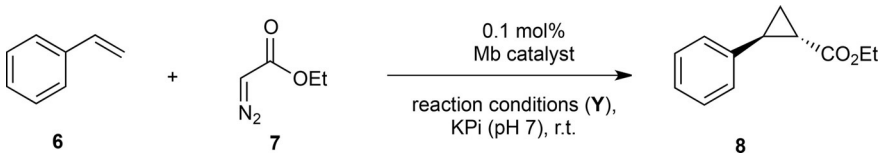

6 **7** **8**

Entry	Catalyst	Cofactor	**Y**[b]	Yield[c]	% *de*[d]	% *ee*[d]
1	Mb(H64V,V68A)	Fe(ppIX)	–/red.	64%	>99	>99
2	Mb(H64V,V68A)	Fe(ppIX)	–/–	14%	71	72
3	Mb(H64V,V68A,H93F)	Fe(ppIX)	–/red.	63%	98	86
4	Mb(H64V,V68A)	Mn(ppIX)	–/red.	29%	>99	99
5	Mb(H64V,V68A)	Co(ppIX)	–/red.	4%	99	99
6	Mb(H64V,V68A)	Ru(CO)(mpIX)	–/red.	7%	42	7
7	Mb(H64V,V68A)	Rh(mpIX)	–/red.	3%	96	97
8	Mb(H64V,V68A)	Ir(Me)(mpIX)	–/red.	25%	56	4
9	Mb(H64V,V68A)	Ir(Me)(mpIX)	–/–	36%	75	0
10	Mb(H64V,V68A)	Fe(ppIX)	O_2/red.	43%	98	95
11	Mb(H64V,V68A,H93F)	Fe(ppIX)	O_2/red.	15%	94	70
12	Mb(H64V,V68A)	Ir(Me)(mpIX)	O_2/–	41%	59	–1
13	Mb(H64V,V68A)	Fe(ppIX)	O_2/red.[e]	68%	>99	>99

[a] *Reaction conditions:* 0.01 M styrene, 0.02 M EDA, 10 μM Mb catalyst, 50 mM phosphate buffer (pH 7) containing 5% ethanol, room temperature.
[b] Variable parameter (**Y**): "–/red."=anaerobic, 0.01 M $Na_2S_2O_4$; "–/–"=anaerobic, no reductant; "O_2-red."=aerobic, 0.01 M $Na_2S_2O_4$; "O_2/–"=aerobic, no reductant.
[c] As determined by gas chromatography (GC) using calibration curves with isolated **8**.
[d] For *trans*-(1*S*,2*S*) stereoisomer as determined by chiral GC.
[e] Using 0.5 mol% catalyst.

the Fe-based variants, for which the H93F substitution has no effect on the catalytic efficiency of the protein (entry 3 *vs.* 1, Table 1). Even if spectroscopically undetectable (Figure 1), the absence of contaminant Mb in the reactions with the cofactor-substituted variants was further confirmed *via* control experiments in which these catalysts were incubated with sodium dithionite and carbon monoxide prior to the reaction.

Other interesting observations were derived from examining the impact of the cofactor and proximal ligand substitutions on the stereoselectivity of the biocatalyst. Indeed, the Mn-containing Mb(H64V,V68A) variant, along with the less active Co- and Rh-containing counterparts, were found to mirror the high stereoselectivity of the Fe-containing Mb(H64V,V68A) variant, producing **8** with high diastereo- and enantioselectivity (96–99% *de*, 97–99% *ee*; entries 4, 5, and 7, Table 1). In contrast, the Mb variants incorporating the Ir(Me)- and Ru(CO)-mesoporphyrin IX cofactors show significantly reduced diastereo- and enantioselectivity under identical reaction conditions (42–56% *de*; 4–7% *ee*; entries 6 and 8, Table 1). These values are similar, albeit not identical, to those exhibited by the free cofactor [e.g., 57% *de*, 0% *ee* for Ir(Me)(mpIX)], raising the question of whether these cofactors are released during the reaction. To address this point, control experiments were conducted using 4-morpholinopyridine, which can bind to Ir(Me)(mpIX) in free form but not when bound to myoglobin.[8a] In the presence of 50 mM 4-morpholinopyridine,[17] negligible product formation was observed in the presence of free Ir(Me)(mpIX), whereas significant amounts of **8** accumulated in the reaction with Mb(H64V,V68A)[Ir(Me)(mpIX)] (i.e., approx. 2-fold lower yield and similar % *de* and *ee* values compared to the reaction with no inhibitor). These results clearly indicate that the observed carbene transfer activity arises from the metalloprotein and not from dissociated cofactor. Since both Ir(Me)(ppIX) and Ru(CO)(ppIX) cofactors bear a metal-bound ligand, we ascribe the low stereoselectivity exhibited by the Ir- and Ru-containing Mb variants compared to the Fe-, Mn-, Co- and Rh-based counterparts to a disruption of the chiral environment provided by the H64V/V68A mutations due to the presence of the axial ligands. This outcome is perhaps not surprising considering that these mutations were selected to favor *trans*-(1*S*,2*S*) selectivity in styrene cyclopropanation with EDA by heme-containing Mb variants which naturally lack a metal-bound ligand.[4a]

As shown by the data in Table 1 and the Supporting Information, Table S2, the stereochemical outcome of the cyclopropanation reaction is also affected by the oxidation state of the metal (entry 2 *vs.* 1, Table 1) and nature of the proximal ligand (entry 3 *vs.* 1, Table 1). For example, the His93Phe substitution significantly affects the enantioselectivity of the Fe-, Mn-, and Co-based Mb variants (48–86% *ee vs.* 99% *ee*). This effect is less pronounced for the Ir- and Ru-based catalysts, likely due to the lack of metal coordination *via* the proximal ligand (*vide infra*). Importantly, the results above demonstrate that the stereoselectivity of these biocatalysts can be affected, and thus tuned, by altering the first coordination sphere and oxidation state of the metal center.

Finally, analysis of the aerobic reactions showed that both Mb(H64V,V68A) and Mb(H64V,V68A)-[Ir(Me)(mpIX)] can furnish the cyclopropanation product **8** in good yields (41–43%) in the presence of oxygen (entries 10 and 12, Table 1). In contrast, the cyclopropanation activity of Mb(H64V,V68A)-[Co(mpIX)] is drastically suppressed under aerobic conditions (<1%, Supporting Information, Table S2). Importantly, the Mb(H64V,V68A)-catalyzed transformation maintains the excellent diastereo- and stereoselectivity observed under anaerobic conditions. Using Mb(H64V,V68A) at 0.5 mol%, the cyclopropanation product **8** was obtained in 68% yield and >99% *de* and *ee* in an open vessel reaction, thus demonstrating the viability of this biocatalytic transformation under aerobic conditions.

N–H Insertion Activity

The carbene N–H insertion reactivity of the Mb catalysts was assessed using the conversion of aniline (**9**) to **10** in the presence of EDA as a model reaction (Table 2 and Supporting Information, Table S3). Similarly to the cyclopropanation reactions, the highest yields in this reaction were obtained with Mb(H64V,V68A) and its related variant bearing the H93F substitution, Mb(H64V,V68A,H93F), under reducing and anaerobic conditions (47–56%, entries 1 and 2, Table 2). At the same time, the differential impact of metal substitution in the N–H insertion reactions compared to cyclopropanation became evident from these data. Indeed, higher N–H insertion activity was observed with Mb catalysts containing first-row metals following the order: Fe > Mn ≈ Co > Rh > Ir ≈ Ru, whereas a different order of reactivity characterized the cyclopropanation reactions (Fe > Mn ≈ Ir > Ru > Rh ≈ Co). Other interesting trends emerged from these experiments. For both types of reactions, the TONs exhibited by the first-row metal-containing Mb catalysts are generally higher (2- to 5-fold) in the presence of reductant (Supporting Information, Tables S2 and S3), indicating that higher catalytic efficiency is provided by lower oxidation states of these metals [i.e., Fe(II)(ppIX) > Fe(III)(ppIX); Co(II)(ppIX) > Co(III)(ppIX), Mn(II)(ppIX) > Mn(III)(ppIX)]. An opposite trend is exhibited by the Mb catalysts incorporating second- and third-row metals, in particular

Table 2. Catalytic activity of cofactor-substituted Mb variants for N–H insertion reaction with aniline and EDA.[a] See the Supporting Information, Table S3 for additional data.

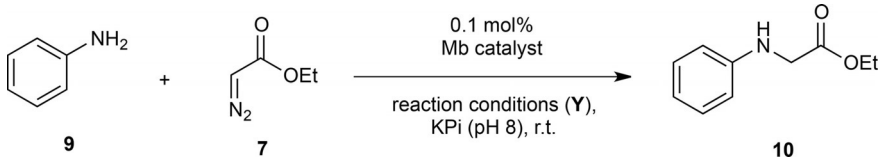

9 7 10

Entry	Catalyst	Cofactor	Y	Yield[b]	TON
1	Mb(H64V,V68A)	Fe(ppIX)	–/red.	56%	555
2	Mb(H64V,V68A,H93F)	Fe(ppIX)	–/red.	47%	467
3	Mb(H64V,V68A)	Mn(ppIX)	–/red.	14%	138
4	Mb(H64V,V68A)	Co(ppIX)	–/red.	13%	129
5	Mb(H64V,V68A)	Ru(CO)(mpIX)	–/red.	5%	52
6	Mb(H64V,V68A)	Rh(mpIX)	–/red.	10%	97
7	Mb(H64V,V68A)	Ir(Me)(mpIX)	–/red.	6%	65
8	Mb(H64V,V68A)	Ir(Me)(mpIX)	–/–	17%	168
9	Mb(H64V,V68A)	Fe(ppIX)	O_2/red.	3%	33
10	Mb(H64V,V68A,H93F)	Fe(ppIX)	O_2/red.	34%	342
11	Mb(H64V,V68A)	Rh(mpIX)	O_2/red.	12%	114
12	Mb(H64V,V68A,H93F)	Fe(ppIX)	O_2/red.[c]	78%	100

[a] *Reaction conditions:* 0.01 M aniline, 0.01 M EDA, 10 μM Mb catalyst, 50 mM phosphate buffer (pH 8) containing 4% ethanol, room temperature. See legend of Table 1 for definition of variable parameter **Y**.
[b] As determined by GC using calibration curves with isolated **10**.
[c] Using 0.75 mol% catalyst.

for the N–H insertion reactions (Supporting Information, Table S3).

Importantly, these experiments led to the successful identification of N–H insertion catalysts capable of operating under aerobic conditions. Specifically, both Mb(H64V,V68A,H93F) and Mb(H64V,V68A,H93F)[Rh(mpIX)] were found to produce **10** in relatively good yields (34% and 12%, respectively) in the presence of oxygen (entries 10 and 11, Table 2). Since Mb(H64V,V68A) shows only minimal product formation (3%) under identical conditions, it can be derived that oxygen tolerance in the Fe-based catalyst is conferred by removal of axial coordination on the heme iron by the proximal residue (entry 9 *vs* 10, Table 2). In contrast, the Rh-based catalyst shows no dependence on the nature of the proximal ligand (Supporting Information, Table S3). Using Mb(H64V,V68A,H93F) at 0.75 mol%, the N–H insertion product **10** was obtained in 78% yield in an open flask reaction (entry 12, Table 2).

S–H Insertion Activity

The carbene S–H insertion reactivity of the metalloproteins was investigated using a model reaction involving thiophenol **11** and EDA to give **12** (Table 3). The results from these experiments further evidenced the peculiar effect of metal and proximal ligand substitution on the carbene transfer reactivity of the Mb catalysts (Table 3 and Supporting Information, Table S4). Under anaerobic conditions, the order of reactivity derived from these data is: Fe > Ir ≈ Ru > Co ≈ Mn > Rh. Thus, whereas the Ru-based Mb variants are poor catalysts for cyclopropanation and N–H insertion reactions (< 1–7% yield, corresponding to < 10–70 TON), they represent effective catalysts for carbene S–H insertion reactions (70–79% yields, corresponding to 700–790 TON). Furthermore, oxygen-tolerant S–H insertion catalysts were identified. In this respect, the best performing Mb variants were determined to be Mb(H64V,V68A,H93F)-[Ir(Me)(mpIX)] (58% yield; entry 11, Table 3), followed by Mb(H64V,V68A)[Ru(CO)(mpIX)] (36% yield) and Mb(H64V,V68A,H93F) (29% yield) (entries 7 and 3, respectively, Table 3). Further substitution of the proximal ligand residue (H93A) in the Ir(Me)-containing variant (*vide infra* for further details) resulted in a catalyst capable of providing quantitative conversion of thiophenol to the desired S–H insertion product **12** in an open vessel reaction (entry 12, Table 3). To examine the role of the protein matrix in influencing the reactivity of the metalloporphyrin cofactors, parallel experiments were conducted using isolated Ir(Me)(mpIX) or Ru(CO)(mpIX) as the catalysts for the S–H insertion reaction under aerobic conditions. These experiments showed that the Ir- and Ru-containing Mb variants exhibit a 3.5-fold and 6-fold higher S–H insertion activity, respectively, compared to corresponding cofactors when

Table 3. Catalytic activity of cofactor-substituted Mb variants for S–H insertion reaction with thiophenol and EDA.[a] See the Supporting Information, Table S4 for additional data.

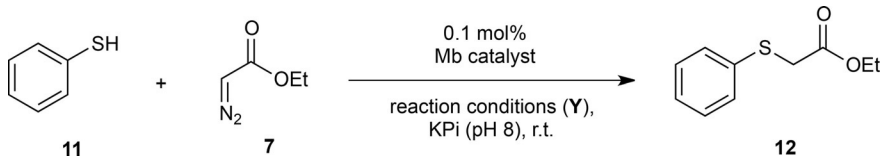

11 7 12

Entry	Catalyst	Cofactor	**Y**	Yield[b]	TON
1	Mb(H64V,V68A)	Fe(ppIX)	–/red.	99%	985
2	Mb(H64V,V68A,H93F)	Fe(ppIX)	–/red.	89%	885
3	Mb(H64V,V68A,H93F)	Fe(ppIX)	O_2/red.	29%	293
4	Mb(H64V,V68A)	Mn(ppIX)	–/red.	13%	133
5	Mb(H64V,V68A)	Co(ppIX)	–/red.	26%	260
6	Mb(H64V,V68A)	Ru(CO)(mpIX)	–/red.	79%	795
7	Mb(H64V,V68A)	Ru(CO)(mpIX)	O_2/–	36%	359
8	Mb(H64V,V68A)	Rh(mpIX)	–/red.	9%	95
9	Mb(H64V,V68A)	Ir(Me)(mpIX)	–/red.	70%	703
10	Mb(H64V,V68A,H93F)	Ir(Me)(mpIX)	–/–	82%	819
11	Mb(H64V,V68A,H93F)	Ir(Me)(mpIX)	O_2/–	58%	579
12	Mb(H64V,V68A,H93A)	Ir(Me)(mpIX)	O_2/–	>99%	>1000

[a] *Reaction conditions:* 0.01 M thiophenol, 0.02 M EDA, 10 μM Mb catalyst, 50 mM phosphate buffer (pH 8) containing 5% ethanol, room temperature. See legend of Table 1 for definition of variable parameter **Y**.
[b] As determined by GC using calibration curves with isolated **12**.

used in free form (Ir: >1,000 *vs.* 290 TON; Ru: 359 *vs.* 59 TON). These results demonstrate the beneficial effect of the protein scaffold toward enhancing the S–H transfer reactivity of the metalloporphyrins.

C–H Insertion Activity

Carbene insertion into C–H bonds constitutes an attractive strategy for C–H functionalization[1c] and seminal works by Callot, Che, and Woo have shown how porphyrin complexes of Rh and Ir can promote these reactions.[16b,18] Inspired by these studies, we hypothesized that metal substitution could provide a potential avenue to endow the Mb catalysts with carbene C–H insertion reactivity. Preliminary experiments indeed showed no detectable C–H insertion activity for the iron-based Mb variants Mb(H64V,V68A) and Mb(H64V,V68A,H93F), as determined using a model reaction with phthalan (**13**) and EDA (Table 4). To our delight, various cofactor-substituted Mb variants were found to produce the desired C–H functionalized product **14** (Table 4). Among them, Mb(H64,V68A)[Co(ppIX)], Mb(H64,V68A,H93F)[Mn(ppIX)], and Mb(H64,V68A)[Ir(Me)(mpIX)] emerged as the most promising catalysts for this transformation, yielding the C–H insertion product **14** in 20–28% yield at a catalyst loading of 0.2 mol% (100–140 TON; entries 7–9, Table 4). Moreover, whereas the catalytic activity of the Ir-containing Mb variant decreases in the presence of oxygen (entry 10 *vs.* 7, Table 4), that of the Co- and Mn-based catalysts slightly increases under aerobic conditions (entries 8–9 *vs.* 2–3, Table 4). Parallel experiments using isolated metalloporphyrins showed that Ir(Me)(mpIX) is a viable, albeit inferior catalyst for this reaction compared to Mb(H64,V68A)[Ir(Me)(mpIX)] (95 *vs.* 140 TON). In contrast, both Mn(ppIX) and Co(ppIX) show negligible C–H insertion reactivity under the same reaction conditions (<5 TON). Altogether, these results highlight the key role of the myoglobin scaffold in endowing the protein-bound Co- and Mn-porphyrins with C–H insertion reactivity.

While this work was in progress, Hartwig and coworkers have reported the directed evolution of an Ir-containing P450 (CYP119) capable of converting **13** to **14** in the presence of EDA (55% yield, 320 TON).[8b] Complementing and extending beyond these findings, the present studies demonstrate the functionality of Ir-substituted Mb variants in promoting an intermolecular carbene C–H insertion reaction. More importantly, our results demonstrate for the first time that artificial metalloproteins incorporating earth-abundant, first-row transition metals (i.e., Co and Mn) can catalyze this challenging transformation. This is particularly noteworthy considering that, as in the case of the aforementioned metalloporphyrins and CYP119(Ir) variants, catalytic systems previously developed for promoting carbene C–H insertions have largely relied on the use of precious metals.[1c,16b,18,19] It is also worth noting that intermolecular C–H insertions in the presence of acceptor-only diazo compounds, such as EDA, have been notoriously dif-

Table 4. Activity of cofactor-substituted Mb variants toward C–H functionalization of phthalan in the presence of EDA.[a] See the Supporting Information, Table S**5** for complete data.

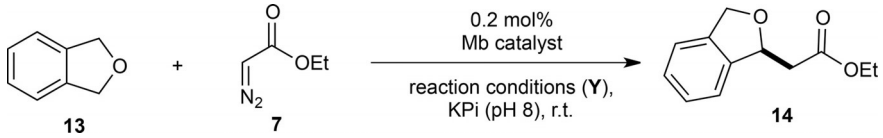

13 7 14

Entry	Catalyst	Cofactor	**Y**	Yield[b]	TON
1	Mb(H64V,V68A)	Fe(ppIX)	–/red.	0%	0
2	Mb(H64V,V68A)	Mn(ppIX)	–/red.	11%	54
3	Mb(H64V,V68A)	Co(ppIX)	–/–	12%	60
4	Mb(H64V,V68A)	Ru(CO)(mpIX)	–/red.	5%	23
5	Mb(H64V,V68A)	Rh(mpIX)	–/red.	12%	59
6	Mb(H64V,V68A)	Ir(Me)(mpIX)	–/red.	16%	80
7	Mb(H64V,V68A)	Ir(Me)(mpIX)	–/–	28%	140
8	Mb(H64V,V68A,H93F)	Mn(ppIX)	O_2/–	20%	101
9	Mb(H64V,V68A)	Co(ppIX))	O_2/–	22%	108
10	Mb(H64V,V68A)	Ir(Me)(mpIX)	O_2/–	20%	98
11	Mb(H64V,V68A,H93A)	Ir(Me)(mpIX)	O_2/–[c]	65%	324

[a] Reaction conditions: 0.01 M phthalan, 0.04 M EDA, 20 μM Mb catalyst, 50 mM phosphate buffer (pH 6) containing 8% ethanol, room temperature. See legend of Table 1 for definition of variable parameter **Y**.
[b] As determined by GC using calibration curves with isolated **14**. Errors are within 10%.
[c] With slow addition of EDA (10 equiv).

ficult, primarily due to the more facile carbene dimerization side reaction competing for the desired C–H insertion process.[19,20] As a result, these transformations have been most effectively carried out in the presence of donor-acceptor diazo reagents, which are less prone to dimerization.[20a,21] In previous studies, we noted how carbene dimerization is largely disfavored in Mb-catalyzed carbene transfer reactions with EDA,[4a,5,6] possibly due to steric protection of the heme-bound carbene intermediate by the protein active site. This feature is likely to provide a beneficial advantage toward favoring the intermolecular carbene C–H insertion reaction documented here. Insights into the enantioselectivity of the Mb-catalyzed C–H insertion reactions described in Table 4 could not be gained at this point due to the difficulty of resolving the enantiomers by chiral GC or SFC. Future studies are thus warranted to further investigate this aspect as well as the scope of these Mb-catalyzed C–H insertion reactions.

Axial Methyl Ligand in Ir(Me)-Myoglobins

The presence of a metal-bound methyl group and carbonyl group in Ir(Me)(mpIX) and Ru(CO)(mpIX), respectively, implies that these axial ligands could occupy either the proximal or distal side of the metalloporphyrin cofactor once the latter is embedded into the protein. Assuming these ligands do not dissociate during catalysis, this aspect has important implications for function since the catalyst configuration with the ligand-free distal site is expected to be sterically more accessible for activating the diazo reagent and thus promoting the carbene transfer reaction. To examine this point, the chemical environment of the Ir-bound methyl group in the Mb catalysts was analyzed by NMR spectroscopy. For the free Ir(Me)(mpIX) cofactor, a single singlet signal corresponding to the methyl ligand is visible at $\delta = -7.78$ ppm (Figure 2A). In contrast, two signals are observed in the same region of the spectrum ($\delta = -8.05$ and -8.17 ppm in $\approx$1:1 ratio) for Mb(H64V,V68A)[Ir(Me)(mpIX)] (Figure 2B). These results are consistent with the presence of two different chemical environments surrounding the methyl group, as given by this group residing on either the "proximal" or the "distal" face of the protein-bound cofactor. The same experiment was carried out with Mb(H64V,V68A,H93F)[Ir(Me)(mpIX)] and Mb(H64V,V68A,H93A)[Ir(Me)(mpIX)], in which different steric demands are imposed at the level of the proximal face of the porphyrin cofactor by virtue of the substitution of His93 with a slightly larger (Phe) or smaller amino acid residue (Ala). Interestingly, the relative intensity of the two signals in the relevant region of the ^{1}H NMR spectra differed significantly for these Mb variants, showing an approximately 20:80 ratio in the presence of the H93F mutation and a 65:35 ratio in the presence of the H93A substitution (Figure 2B). These results thus support a direct effect of the proximal residue on the relative abundance of the two possible catalyst configurations as relative to the orientation of the methyl axial ligand. Whereas a definite assignment cannot be

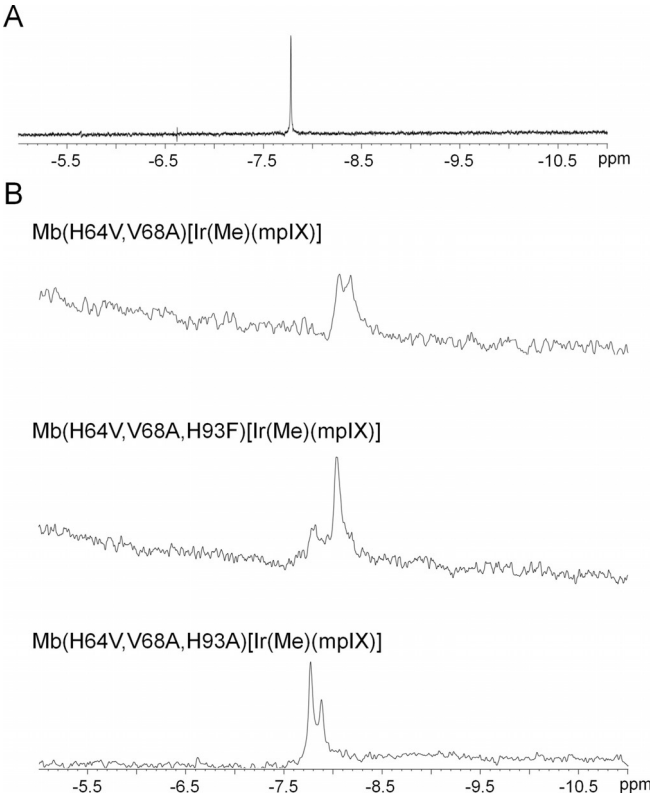

Figure 2. Partial ^{1}H NMR spectra corresponding to (**A**) free Ir(Me)-mesoporphyrin IX, and (**B**) the three Ir(Me)-containing variants. This region of the spectrum shows the signal(s) corresponding to the Ir-bound methyl group.

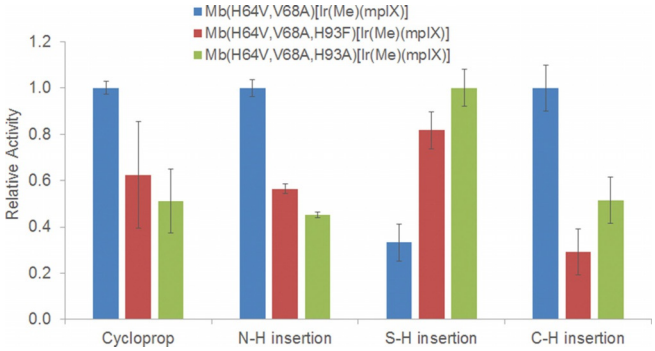

Figure 3. Relative activity of H93 variants of Ir(Me)-containing Mb catalysts across different carbene transfer reactions. For each reaction, activity is normalized to that of the most active variant (cycloprop.: 356 TON; N–H insert.: 168 TON; S–H insert.: 1,000 TON; C–H insert.: 140 TON). Reactions conditions are as described in Tables 1–4 with **Y** = anaerobic, no reductant.

made on the basis of these data alone, steric arguments suggest that the predominant species in the H93A variant could correspond to that in which the Ir-bound methyl group is located on the proximal face of the protein-bound cofactor.

To examine the impact of the H93A mutation on catalytic function, Mb(H64V,V68A,H93A)[Ir(Me)-(mpIX)] was characterized for its activity toward the various carbene transfer reactions discussed earlier. Interestingly, this Mb variant was found to exhibit similar or slightly lower TON in the cyclopropanation, N–H insertion, and C–H insertion reactions when compared to Mb(H64V,V68A)[Ir(Me)(mpIX)] or Mb(H64V,V68A,H93F)[Ir(Me)(mpIX)] (Figure 3). The orders of reactivity emerging from these experiments are His > Phe ≈ Ala for cyclopropanation, His > Phe > Ala for N–H insertion, and His > Ala > Phe for C–H insertion. Departing from this trend are the S–H insertion reactions, in which the Ala93 containing variant consistently exhibits higher performance than the His93 and Phe93 counterparts under the different reaction conditions (Ala > Phe ≫ His; Supporting Information, Table S4). Furthermore, the C–H insertion reaction catalyzed by Mb(H64V,V68A,H93A)[Ir(Me)(mpIX)] could be applied to obtain **14** in 65% yield (entry 11, Table 4), suggesting a higher stability of this variant as compared to the related variants containing Phe or His at the proximal site.

Altogether, these results reveal an interesting and complex role of the proximal ligand on modulating the carbene transfer reactivity of these metalloproteins. Although the H93A mutations is likely to favor a catalyst configuration with an open distal side, this translates in superior catalytic performance for only one of the four different carbene transfer reactions investigated here. Thus, it is possible that electronic and/or steric effects imposed by bulkier proximal residues could provide an advantage in terms of reactivity for the sterically disfavored species bearing the methyl ligand in the proximal side. While further studies are warranted to elucidate this aspect in more detail, it is anticipated that these structure–activity insights will aid the future design and development of hemoprotein-based artificial enzymes incorporating non-natural cofactors, and especially those bearing metal-bound ligands.

Conclusions

In summary, this work demonstrates how modification of the cofactor environment constitutes an effective strategy to modulate and expand the reactivity of myoglobin-based carbene transfer catalysts. In particular, our results show how the catalytic activity, stereoselectivity, and oxygen tolerance of this metalloprotein in various carbene transfer reactions can be tuned by varying the nature of the metal, its oxidation state, and first-sphere coordination by the proximal histidine residues. Of note, this approach proved effective in obtaining Mb catalysts capable of promoting cyclopropanation, S–H and N–H insertion reactions under

aerobic conditions, which is expected to enhance the accessibility and operational simplicity of these carbene transfer biocatalysts for synthetic applications. Importantly, it also enabled expansion of the reaction scope of engineered myoglobins to include intermolecular carbene C–H insertion. In this regard, the demonstrated reactivity of the Co- and Mn-based myoglobins toward carbene C–H insertions is particularly noteworthy, as previously reported catalytic systems useful for this type of carbene transfer reactions have typically relied on the use of rare and expensive transition metals. Finally, another relevant contribution of the present work is the implementation of a simple and technically straightforward strategy for the recombinant production of hemoprotein-based catalysts bearing non-native metalloporphyrin cofactors, also including second- and third-row transition metal centers, in bacterial cells. These advances are expected to facilitate the application of these artificial enzymes in whole cell systems and pave the way to the integration of carbene-mediated transformations into biosynthetic pathways in living organisms. Work in these directions is currently ongoing in our laboratory.

Experimental Section

Reagents

All chemicals and reagents were purchased from commercial suppliers (Sigma–Aldrich, Alfa Aesar) and used without any further purification, unless otherwise stated. Mn- and Co-protoporphyrin IX, protoporphyrin IX dimethyl ester, and mesoporphyrin IX dimethyl ester were purchased from Frontier Scientific. EDA was purchased from Sigma–Aldrich as 87% solution in dichloromethane. All dry reactions were carried out under argon or nitrogen in oven-dried glassware with magnetic stirring using standard gas-tight syringes, cannulae and septa. ^{1}H and ^{13}C NMR spectra were measured on Bruker DPX-400 (operating at 400 MHz for ^{1}H and 100 MHz for ^{13}C) or Bruker DPX-500 (operating at 500 MHz for ^{1}H and 125 MHz for ^{13}C) instruments. Tetramethylsilane (TMS) (0 ppm) or D_2O (4.6 ppm) or DMSO-d_6 (2.50 ppm) served as the internal standard for ^{1}H NMR and $CDCl_3$ (77.0 ppm) or DMSO-d_6 (39.51 ppm) was used as the internal standard for ^{13}C NMR. Silica gel chromatography purifications were carried out using AMD Silica Gel 60 230–400 mesh. Alumina chromatography purifications were carried out using Fisher Scientific Alumina 80–200 mesh. Thin layer chromatography (TLC) and preparative TLC were carried out using Merck Millipore TLC silica gel 60 F254 glass plates.

Analytical Methods

Gas chromatography (GC) analyses were carried out using a Shimadzu GC-2010 gas chromatograph equipped with an FID detector and a Chiral Cyclosil-B column (30 m × 0.25 mm × 0.25 μm film). Separation method for cyclopropanation reaction: 1 μL injection, injector temp.: 200 °C, detector temp.: 300 °C. Gradient: column temperature set at 120 °C for 3 min, then to 150 °C at 0.8 °C min^{-1}, then to 245 °C at 25 °C min^{-1}. Total run time was 46.30 min. Separation method for N–H insertion reaction, S–H insertion reaction and C–H insertion reaction: 1 μL injection, injector temp.: 200 °C, detector temp.: 300 °C. Gradient: column temperature set at 140 °C for 3 min, then to 160 °C at 1.8 °C min^{-1}, then to 165 °C at 1 °C min^{-1}, then to 245 °C at 25 °C min^{-1}. Total run time was 28.31 min.

Growth Media

Cell cultures were grown in enriched M9 medium which was prepared as follows. For 1 L, 770 mL deionized H_2O were mixed with 200 mL M9 salts (5×) solution, 20 mL glucose (20% v/v), 10 mL casamino acids (20% m/v), 1 mL $MgSO_4$ (2 M), and 100 μL $CaCl_2$ (1 M). The M9 salts (5×) solution was prepared by dissolving 15 g Na_2HPO_4, 7.5 g K_2HPO_4, 0.3 g NaH_2PO_4, 0.3 g KH_2PO_4, 1.5 g NaCl, 5 g NH_4Cl in 2 L deionized H_2O and sterilized by autoclaving. The casamino acids and $MgSO_4$ solutions were autoclaved separately. The $CaCl_2$ and glucose stock solutions were sterilized by filtration. Enriched M9 agar plates were prepared by adding 17 g agar to 1 L of enriched M9 media containing all of the aforementioned components at the specified concentrations with the exception of glucose and $CaCl_2$, which were added immediately prior to plating. To media and plates, ampicillin was added to a final concentration of 100 mg L^{-1} and chloramphenicol was added to a final concentration of 34 mg L^{-1}.

Expression of Cofactor-Substituted Myoglobin Variants

The Mb variants were expressed from pET22-based vectors[14] containing the protein gene under a T7 promoter. The recombinant protein contains a C-terminal poly-histidine tag. The heme transporter ChuA and GroES/EL proteins were expressed from a pACYC-based plasmid (pGroES/EL-ChuA), in which the *ChuA* gene is under the control of a T7 promoter and the *GroES/EL* genes are under the control of an araBAD promoter.[14] *E. coli* C41(DE3) cells were co-transformed with the pGroES/EL-ChuA plasmid and the pET22 vector for expression of the desired Mb variant and selected on M9 agar plates containing ampicillin (100 mg L^{-1}) and chloramphenicol (34 mg L^{-1}). Single colonies of the co-transformed cells were used to inoculate 5 mL overnight cultures of enriched M9 media (37 °C, 150 rpm, 12 hours). The overnight cultures were used to inoculate 1 L of enriched M9 medium. When OD_{600} reached 1.4, cell cultures were condensed by centrifugation (4,000 rpm, 4 °C, 20 min) followed by resuspension of the cell pellet in 200 mL of enriched M9 medium. A 6 mg sample of solid cofactor was dissolved in 50 μL of DMSO or less. The cofactor solution was added directly to the condensed expression culture. In addition, arabinose was added to a final concentration of 4 mM L^{-1} from a 0.4 M stock solution. The expression culture was shaken at 37 °C and 150 rpm for 30 minutes before induction with IPTG (final concentration 0.5 mM L^{-1}) from a 0.5 M stock solution. The induced culture was shaken at 20 °C and 150 rpm for additional 16 to 20 hours. The cells were pelleted by centrifugation (4,000 rpm, 4 °C, 20 min) and then resuspended in

20 mL of Ni-NTA Lysis Buffer (50 mM KPi, 250 mM NaCl, 10 mM histidine, pH 8.0). Resuspended cells were frozen and stored at −80 °C until purification.

Protein Purification

Cell suspensions were thawed at room temperature, lysed by sonication, and clarified by centrifugation (14,000 rpm, 20 min, 4 °C). The clarified lysate was transferred to a Ni-NTA column equilibrated with Ni-NTA Lysis Buffer. The resin was washed with 50 mL of Ni-NTA Lysis Buffer and then 50 mL of Ni-NTA Wash Buffer (50 mM KPi, 250 mM NaCl, 20 mM histidine, pH 8.0). Proteins were eluted with Ni-NTA Elution Buffer (50 mM KPi, 250 mM NaCl, 250 mM histidine, pH 7.0). After elution from the Ni-NTA column, the protein was buffer exchanged against 50 mM KPi buffer (pH 7.0) using 10 kDa Centricon filters. The concentration of the Mb variants was determined using the following extinction coefficients: $\varepsilon_{410} = 157\ mM^{-1}cm^{-1}$ for Fe(ppIX)-containing variants; $\varepsilon_{470} = 60\ mM^{-1}cm^{-1}$ for Mn(ppIX)-containing variants; $\varepsilon_{424} = 152.5\ mM^{-1}cm^{-1}$ for Co(ppIX)-containing variants; $\varepsilon_{398} = 395\ mM^{-1}cm^{-1}$ for Ru(CO)(mpIX)-containing variants; $\varepsilon_{405} = 122\ mM^{-1}cm^{-1}$ for Rh(mpIX)-containing variants; and $\varepsilon_{400} = 117.5\ mM^{-1}cm^{-1}$ for Ir(Me)(mpIX)-containing variants.

Expression and Purification of Apomyoglobin

BL21(DE3) cells were transformed with the pET22-based vector encoding for the appropriate Mb variant and transformed cells were selected on enriched M9 agar plates containing ampicillin (100 mg L^{-1}). Single colonies were used to inoculate 5 mL of enriched M9 media supplemented with ampicillin (100 mg L^{-1}), followed by incubation at 37 °C with shaking (180 rpm) for 10 to 15 hours. The overnight cultures were transferred to 1 L enriched M9 medium containing ampicillin, followed by incubation at 37 °C with shaking (180 rpm). At an OD_{600} of 1.4, cells were induced with IPTG (final conc.: 0.5 mM) and incubated at 20 °C with shaking (180 rpm) for 20 to 24 hours. Cells were harvested by centrifugation (4,000 rpm, 4 °C, 20 minutes). Cell pellets were resuspended in 20 mL of Ni NTA Lysis Buffer (50 mM KPi, 250 mM NaCl, 10 mM histidine, pH 8.0) and stored at −80° C until purification. Apomyoglobin was purified using the protocol described above. After elution from the Ni-NTA column, the protein was buffer exchanged against 50 mM KPi buffer (pH 7.0) using 10 kDa Centricon filters. The apomyoglobin variants were stored at 4 °C for no longer than 12 hours.

Chemical Synthesis

Synthetic procedures and characterization data for the metalloporphyrins Ir(CO)Cl protoporphyrin dimethyl ester, Ir(Me)-protoporphyrin IX, Ir(CO)Cl mesoporphyrin dimethyl ester, Ir(Me) mesoporphyrin IX, Rh mesoporphyrin IX, Ru(CO)-mesoporphyrin IX dimethyl ester, Ru(CO)-mesoporphyrin IX as well as the enzymatic synthesis of ethyl 2-(1,3-dihydroisobenzofuran-1-yl)acetate **14** are provided in the Supporting Information.

Reconstitution of Apomyoglobin with Non-native Cofactors

Stock solutions of the desired cofactor (5 mg mL^{-1} in DMSO) were added to a solution of apomyoglobin variant (300–800 μM) in order to achieve an apomyoglobin:cofactor molar ratio of 2 to 1. Special care was taken so that the final concentration of DMSO in the apomyoglobin solution did not exceed 2% v/v. Reconstitution mixtures were incubated for 5 min on ice after mixing. Unbound cofactor was separated from the reconstituted protein using a NAP-10 desalting column equilibrated with 50 mM KPi (pH 7).

Cyclopropanation, N–H Insertion, and S–H Insertion Reactions

Reactions with styrene, aniline, and thiophenol were carried out as described previously.[4a,5] Briefly, under standard reaction conditions, reactions were carried out at a 400 μL scale using 10 μM Mb variant, 10 mM styrene (or thiophenol or aniline), 20 mM EDA (10 mM for N–H insertion), and 10 mM sodium dithionite. In a typical procedure, a solution containing sodium dithionite (100 mM stock solution) in potassium phosphate buffer (50 mM, pH 7.0, pH 8.0 for S–H and N–H insertions) was degassed by bubbling argon into the mixture for 4 min in a sealed vial. A buffered solution containing myoglobin was carefully degassed in a similar manner in a separate vial. The two solutions were then mixed together *via* cannula. Reactions were initiated by addition of 10 μL of styrene or thiophenol or aniline (from a 0.4 M stock solution in ethanol), followed by the addition of 10 μL of EDA (5 μL for N–H insertion) (from a 0.8 M stock solution in ethanol) with a syringe, and the reaction mixture was stirred for 16 hours at room temperature, under positive argon pressure. Reactions without reductant were performed in a similar manner without the addition of sodium dithionite. Aerobic reactions were carried out without degassing the solutions with argon and in open vessels.

C–H Insertion Reactions

Under standard reaction conditions, reactions were carried out at a 400 μL scale using 20 μM Mb variant, 10 mM phthalan, 40 mM EDA, and 10 mM sodium dithionite. In a typical procedure, a solution containing sodium dithionite (100 mM stock solution) in potassium phosphate buffer (50 mM, pH 6.0) was degassed by bubbling argon into the mixture for 4 min in a sealed vial. A buffered solution containing myoglobin was carefully degassed in a similar manner in a separate vial. The two solutions were then mixed together *via* cannula. Reactions were initiated by addition of 10 μL of phthalan (from a 0.4 M stock solution in ethanol), followed by the addition of 20 μL of EDA (from a 0.8 M stock solution in ethanol) with a syringe, and the reaction mixture was stirred for 14 hours at room temperature, under positive argon pressure. Reactions without reductant were performed in a similar manner without the addition of sodium dithionite and aerobic reactions were carried out without solution degassing with argon.

For optimized conversion, reactions were carried out at a 1 mL scale using 20 μM Mb variant, 10 mM phthalan and 100 mM EDA. In a typical procedure, potassium phosphate buffer (50 mM, pH 6.0) was degassed by bubbling argon

into the mixture for 4 min in a sealed vial. A buffered solution containing myoglobin was carefully degassed in a similar manner in a separate vial. The two solutions were then mixed together *via* cannula. Reactions were initiated by addition of 10 μL of phthalan (from a 1 M stock solution in DMF), followed by the addition of 20 μL of EDA (from a 5 M stock solution in DMF) with a syringe pump over a period of 1–2 hours, and the reaction mixture was stirred for 2 hours at room temperature, under positive argon pressure.

Product Analysis

The cyclopropanation, S–H insertion, N–H insertion and C–H insertion reactions were analyzed by adding 20 μL of internal standard (benzodioxole, 50 mM in ethanol) to the reaction mixture, followed by extraction with 400 μL of dichloromethane and analysis by GC-FID (see Analytical Methods section for details on GC analyses). C–H insertion reaction (with slow addition of EDA) was analyzed by adding 40 μL of internal standard (benzodioxole, 50 mM in ethanol) to the reaction mixture, followed by addition of 200 μL of saturated sodium chloride solution, extraction with 800 μL of ethyl acetate, and analysis by GC-FID (see Analytical Methods section for details on GC analyses). Calibration curves for quantification of the S–H insertion, N–H insertion, and cyclopropanation products were constructed using authentic (racemic) standards prepared synthetically or enzymatically as described previously.[4a,5] Authentic standards for the C–H insertion reactions were prepared as described in the Supporting Information. All measurements were performed at least in duplicate. For each experiment, negative control samples containing no enzyme were included.

NMR Experiments

The ^{1}H NMR experiments were carried out using a Bruker-DPX-500 spectrometer and solutions of the three Ir(Me)(m-pIX)-containing myoglobin variants (0.35–0.55 mM) in potassium phosphate buffer (50 mM, pH 7.0) containing 10% D_2O. ^{1}H NMR spectra were calibrated using the solvent (water) peak as reference.

Acknowledgements

This work was supported in part by the U.S. National Institute of Health grant GM098628 and in part by the National Science Foundation grant CHE-1609550. MS instrumentation was supported by the U.S. NSF grant CHE-0946653.

References

[1] a) A. Padwa, M. D. Weingarten, *Chem. Rev.* **1996**, *96*, 223–269; b) M. P. Doyle, D. C. Forbes, *Chem. Rev.* **1998**, *98*, 911–936; c) H. M. L. Davies, R. E. J. Beckwith, *Chem. Rev.* **2003**, *103*, 2861–2903; d) H. Lebel, J. F. Marcoux, C. Molinaro, A. B. Charette, *Chem. Rev.* **2003**, *103*, 977–1050; e) Z. H. Zhang, J. B. Wang, *Tetrahedron* **2008**, *64*, 6577–6605; f) M. M. Diaz-Requejo, P. J. Perez, *J. Organomet. Chem.* **2005**, *690*, 5441–5450; g) H. Pellissier, *Tetrahedron* **2008**, *64*, 7041–7095; h) S. F. Zhu, Q. L. Zhou, *Acc. Chem. Res.* **2012**, *45*, 1365–1377; i) D. Gillingham, N. Fei, *Chem. Soc. Rev.* **2013**, *42*, 4918–4931.

[2] a) H. Renata, Z. J. Wang, F. H. Arnold, *Angew. Chem.* **2015**, *127*, 3408–3426; *Angew. Chem. Int. Ed.* **2015**, *54*, 3351–3367; b) T. Heinisch, T. R. Ward, *Eur. J. Inorg. Chem.* **2015**, 3406–3418; c) J. G. Gober, E. M. Brustad, *Curr. Opin. Chem. Biol.* **2016**, *35*, 124–132.

[3] a) P. S. Coelho, E. M. Brustad, A. Kannan, F. H. Arnold, *Science* **2013**, *339*, 307–310; b) P. S. Coelho, Z. J. Wang, M. E. Ener, S. A. Baril, A. Kannan, F. H. Arnold, E. M. Brustad, *Nat. Chem. Biol.* **2013**, *9*, 485–487; c) H. Renata, Z. J. Wang, R. Z. Kitto, F. H. Arnold, *Catal. Sci. Technol.* **2014**, *4*, 3640–3643; d) Z. J. Wang, N. E. Peck, H. Renata, F. H. Arnold, *Chem. Sci.* **2014**, *5*, 598–601; e) Z. J. Wang, H. Renata, N. E. Peck, C. C. Farwell, P. S. Coelho, F. H. Arnold, *Angew. Chem.* **2014**, *126*, 6928–6931; *Angew. Chem. Int. Ed.* **2014**, *53*, 6810–6813.

[4] a) M. Bordeaux, V. Tyagi, R. Fasan, *Angew. Chem.* **2015**, *127*, 1746–1748; *Angew. Chem. Int. Ed.* **2015**, *54*, 1744–1748; b) P. Bajaj, G. Sreenilayam, V. Tyagi, R. Fasan, *Angew. Chem. Int. Ed.* **2016**, *55*, 16110–16114; c) A. Tinoco, V. Steck, V. Tyagi, R. Fasan, *J. Am. Chem. Soc.* **2017**, *139*, 5293–5296.

[5] a) G. Sreenilayam, R. Fasan, *Chem. Commun.* **2015**, *51*, 1532–1534; b) V. Tyagi, R. B. Bonn, R. Fasan, *Chem. Sci.* **2015**, *6*, 2488–2494.

[6] V. Tyagi, R. Fasan, *Angew. Chem.* **2016**, *128*, 2558–2562; *Angew. Chem. Int. Ed.* **2016**, *55*, 2512–2516.

[7] V. Tyagi, G. Sreenilayam, P. Bajaj, A. Tinoco, R. Fasan, *Angew. Chem.* **2016**, *128*, 13760–13764; *Angew. Chem. Int. Ed.* **2016**, *55*, 13562–13566.

[8] a) H. M. Key, P. Dydio, D. S. Clark, J. F. Hartwig, *Nature* **2016**, *534*, 534–537; b) P. Dydio, H. M. Key, A. Nazarenko, J. Y. Rha, V. Seyedkazemi, D. S. Clark, J. F. Hartwig, *Science* **2016**, *354*, 102–106.

[9] a) P. Srivastava, H. Yang, K. Ellis-Guardiola, J. C. Lewis, *Nat. Commun.* **2015**, *6*, 7789; b) J. G. Gober, A. E. Rydeen, E. J. Gibson-O'Grady, J. B. Leuthaeuser, J. S. Fetrow, E. M. Brustad, *Chembiochem* **2016**, *17*, 394–397; c) E. W. Reynolds, M. W. McHenry, F. Cannac, J. G. Gober, C. D. Snow, E. M. Brustad, *J. Am. Chem. Soc.* **2016**, *138*, 12451–12458; d) A. Rioz-Martinez, J. Oelerich, N. Segaud, G. Roelfes, *Angew. Chem.* **2016**, *128*, 14342–14346; *Angew. Chem. Int. Ed.* **2016**, *55*, 14136–14140.

[10] F. Yang, G. N. Phillips, *J. Mol. Biol.* **1996**, *256*, 762–774.

[11] a) T. Yonetani, T. Asakura, *J. Biol. Chem.* **1969**, *244*, 4580–4588; b) T. Hayashi, H. Dejima, T. Matsuo, H. Sato, D. Murata, Y. Hisaeda, *J. Am. Chem. Soc.* **2002**, *124*, 11226–11227; c) T. Matsuo, T. Hayashi, Y. Hisaeda, *J. Am. Chem. Soc.* **2002**, *124*, 11234–11235; d) H. Sato, M. Watanabe, Y. Hisaeda, T. Hayashi, *J. Am. Chem. Soc.* **2005**, *127*, 56–57; e) K. Oohora, Y. Kihira, E. Mizohata, T. Inoue, T. Hayashi, *J. Am. Chem. Soc.* **2013**, *135*, 17282–17285.

[12] N. Kawakami, O. Shoji, Y. Watanabe, *Chembiochem* **2012**, *13*, 2045–2047.

[13] C. L. Varnado, D. C. Goodwin, *Protein Expres. Purif.* **2004**, *35*, 76–83.
[14] M. Bordeaux, R. Singh, R. Fasan, *Bioorg. Med. Chem.* **2014**, *22*, 5697–5704.
[15] V. S. Lelyveld, E. Brustad, F. H. Arnold, A. Jasanoff, *J. Am. Chem. Soc.* **2011**, *133*, 649–651.
[16] a) B. J. Anding, A. Ellern, L. K. Woo, *Organometallics* **2012**, *31*, 3628–3635; b) B. J. Anding, J. Brgoch, G. J. Miller, L. K. Woo, *Organometallics* **2012**, *31*, 5586–5590; c) B. J. Anding, L. K. Woo, *Organometallics* **2013**, *32*, 2599–2607.
[17] In our hands, 4-morpholinopyridine at 1 mM failed to inhibit the Ir(Me)(mpIX)-catalyzed cyclopropanation of styrene with EDA as reported in ref.[8a] A concentration of 50 mM of this inhibitor was found to be optimal for inducing full inhibition of free Ir(Me)(mpIX), while resulting in only partial inhibition of Ir(Me)(mpIX)-containing Mb.
[18] a) H. J. Callot, F. Metz, *Tetrahedron Lett.* **1982**, *23*, 4321–4324; b) J. C. Wang, Z. J. Xu, Z. Guo, Q. H. Deng, C. Y. Zhou, X. L. Wan, C. M. Che, *Chem. Commun.* **2012**, *48*, 4299–4301.
[19] N. M. Weldy, A. G. Schafer, C. P. Owens, C. J. Herting, A. Varela-Alvarez, S. Chen, Z. Niemeyer, D. G. Musaev, M. S. Sigman, H. M. L. Davies, S. B. Blakey, *Chem. Sci.* **2016**, *7*, 3142–3146.
[20] a) L. T. Scott, G. J. Decicco, *J. Am. Chem. Soc.* **1974**, *96*, 322–323; b) A. Demonceau, A. F. Noels, A. J. Hubert, P. Teyssie, *J. Chem. Soc. Chem. Commun.* **1981**, 688–689; c) M. M. Diaz-Requejo, T. R. Belderrain, M. C. Nicasio, S. Trofimenko, P. J. Perez, *J. Am. Chem. Soc.* **2002**, *124*, 896–897; d) H. V. R. Dias, R. G. Browning, S. A. Richey, C. J. Lovely, *Organometallics* **2004**, *23*, 1200–1202.
[21] H. M. L. Davies, T. Hansen, M. R. Churchill, *J. Am. Chem. Soc.* **2000**, *122*, 3063–3070.

